Impact of thermal treatment on bentonite retention ability towards nickel and silver retention

Y. El Ouardi, C. Branger, K. Laatikainen, G. Durrieu, S. Mounier, A. Ouammou, V. Lenoble

Impact of thermal treatment on bentonite retention ability towards nickel and silver retention

Y. El Ouardi [a-b-c*], C. Branger [b], K. Laatikainen [d], G. Durrieu [a], S. Mounier [a], A. Ouammou [c], V. Lenoble.[a*]

[a]*Université de Toulon, Aix Marseille Univ, CNRS, IRD, MIO, France*

[b]*Université de Toulon, MAPIEM, Toulon, France*

[c]*Université Sidi Mohamed Ben Abdellah, Faculté des Sciences Dhar El Mehraz, LIMOM Laboratory, Dhar El Mehraz B.P. 1796 Atlas, Fès 30000, Morocco*

[d]*Lappeenranta-Lahti University of Technology, Laboratory of Computational and Process Engineering, P.O. Box 20, FI-53851 Lappeenranta, Finland*

***Corresponding authors:**
E-mail addresses:uceef.elouardi@gmail.com (Y. El Ouardi), lenoble@univ-tln.fr (V. Lenoble).

Abstract

In this work, a natural bentonite was submitted to heating treatment (at 550 and 750°C) in order to correlate such treatment to an improvement of the metal adsorption properties. The characterization of all materials includes XRD, FTIR, TGA, SEM analysis and porosity measurements. The efficiency of raw and calcined bentonite to remove nickel and silver from aqueous solution was highlighted and fell in the upper range when compared to material of similar composition taken from the literature. Raw and bentonite calcined at 550 °C properties towards metal retention remained in such upper range of efficiency when tested in complex effluents like industrials wastewaters.

Keywords: bentonite, thermal treatment, adsorption, nickel, silver.

Introduction

Bentonite, a natural colloidal clay is a widespread material. [1] Bentonites are mainly composed of montmorillonite, $(Na,Ca)_{0.3}(Al, Mg)_2Si_4O_{10}(OH)_2.n(H_2O)$ [2], with a small amount of other clay minerals. They have wide range of applications in different industrial fields such as drilling, molding, ceramics, paint, pharmaceutical or bleaching earths [3]. Most of the bentonite exploited in the world is used as a binder of molding sand in the molding industry and also to thicken drilling fluids. [3–6]. Bentonites are also

widely used in geotechnical applications throughout the world because these clay materials possess advantageous properties such as a high cation exchange capacity, small particles size compared to other clay minerals like illite and kaolinite, and low permeability. [7] Because of their economic benefits, as they are low-cost and abundant natural materials, and because of their intrinsic properties such as high surface area, excellent physical and chemical stability and other structural and surface properties, bentonites' use has been recently extended also to removal of toxic metals in effluents. [1, 8] Bentonite is therefore added to the list of material used to remediate a contaminated effluent. In spite of these interesting properties, there is an everlasting desire to develop new adsorbents or to increase the retention potential of the existing ones.

In order to enhance and improve adsorbent properties, materials can undergo different modifications including acid activation [9], treatment with cationic surfactants [10], modification with polymer [11] and heat treatment. [12] Yet, according to the considered materials, the obtained results do not always follow a clear trend. Concerning bentonite enhancement, its modification by grafting of cationic surfactant molecules will lead to the transformation of the initial hydrophilic character into a hydrophobic and organophilic one and thus an increase in the basal distance [10]. Another modification of bentonite is activation with concentrated acids such as sulfuric acid at a high temperature, which increases the surface acidity, leading to the deep destruction of the crystal lattice, the increase of the specific surface and of the number of active sites. [9] Yet, acid treatment was demonstrated to lead to a less important bentonite structural modification compared to thermal treatment. [12–14] Among the studies related to thermal treatment, the adsorption efficiency before and after heating treatment was not

systematically performed, when it is the principle of the approach developed in this study.

In the present work, a natural bentonite from northeastern Morocco was studied and fully characterized as raw bentonite but also after thermal treatment at 550 and 750 °C. The various materials were then compared for their retention efficiency.

Unusually high nickel and silver concentrations are encountered in a river within a touristic area of Morocco. This contamination results from brassware production, an important economic sector as well as a traditional activity in Moroccan society. Due to their antibacterial efficiency, nickel and silver presence in the water leads to the degradation of the system used in the nearby local wastewater treatment plant. Therefore, there is an urgent need for a preliminary adsorption step allowing an efficient metal removal upstream of the treatment plant. Thus, the aim of this study was to evaluate the potential of raw bentonite as well as the calcinated materials for adsorptive removal of nickel and silver ions from real wastewater samples. ~~The raw bentonite as well as the calcinated materials were consequently tested for their adsorption efficiency over these two contaminants. Nickel and silver were considered in a matrix of increasing complexity to finally be tested in natural effluents: river water as well as effluents from brassware industry~~. In view of a potential industrial process, the material regeneration was also checked and guaranteed.

Materials and Methods

Solids preparation

In this study, a natural bentonite was sampled in Trebia deposit in northeastern Morocco. The raw bentonite was sieved and the fraction below 100 µm was collected. Then, the material was separated in different portions (around 200 g each), which were

subsequently calcined under air atmosphere at two different final temperatures: 550 and 750 °C, in a programmable electric furnace (Nabertherm LHT-08/17, Germany) applying a heating rate of 5 °C/min, from room temperature to the selected calcination temperature. The samples were left in the furnace for 6 hours at the calcination temperature before cooling with a constant cooling rate of 5 °C/min. The obtained materials will hereafter be labelled as raw-Be for untreated bentonite, Be550 and Be750 for bentonite treated at 550 and 750 °C, respectively.

Solids characterization

The pH of the dispersions formed by the bentonite (as raw and calcined materials) was directly measured in a 1:100 solid to liquid ratio aqueous extract, i.e., on 0.1 g of sample dispersed in 10 mL of milliQ water (initial pH of 5.5).

Organic carbon in samples was determined with a Thermal Scientific Flash 2000 NC Soil Analyzer. A mass of 12 mg of sample was placed in a tin capsule. Carbon was measured by flash combustion at 930 °C. Carbon content in sample is converted in CO_2, further separated from other combustion gases in a chromatographic column and detected with a thermal conductivity detector. The limit of detection was respectively 5 µg for C and the calibration curve ranges from 10 to 1100 µg for C.

The zeta potential (ZP) measurements were realized using a Zetasizer Nano ZS (Malvern Instruments).

Powder X-ray diffraction (XRD) patterns of the samples were obtained with a X'Pert Pro panalytical diffractometer using a CuK_α radiation at 40 kV and 30 mA with a scan range of 5–70 °2θ, a scan speed of 0.02 °2θ per 2s, and a step size of 0.02 °2θ.

Fourier-Transform InfraRed (FTIR) spectra were obtained on a Bruker Vertex70 spectrometer equipped with a D-LaTGS-detector (L-alanine doped triglycine sulfate).

About 1 mg of sample was mixed with approximately 300 mg of dried KBr and pressed to get pellets. The measurements were carried out over the range 4000–400 cm^{-1} in the transmittance mode, with a spectral resolution of 4 cm^{-1}.

Themogravimetric analysis (TGA) was obtained on a SDT-TGA Q600. Samples (approximately 10 mg) were inserted in ceramic pans submitted to heating (10 °C/min heating rate) from 30 °C to 1000 °C in a flowing air atmosphere of 100 mL/min.

For scanning electron microscopy (SEM), samples were covered with gold and microscopy was performed using a scanning electron microscope (Zeiss-Supra 40 VP/Gemini Column) with 1500 X zoom for each sample.

The specific surface areas were determined according to the Brunauer Emmet–Teller (BET) equation with nitrogen adsorption–desorption isotherms at 77 K using a Micrometrics Gemini V apparatus.

Reagents

MilliQ water (resistivity 18.2 MΩ, TOC < 10 µg/L, Millipore, Milli-Q system) was used to prepare all the solutions mentioned below. Nickel (II) nitrate hexahydrate (99.9 %, $Ni(NO_3)_2.6H_2O$), was used as received from Sigma Aldrich. Ag(I) Silver nitrate (≥99.7 %, $Ag(NO_3)$) was purchased from Fisher Scientific (Analytical Grade). N-(2-hydroxyethyl) piperazine-N-2-ethanesulfonic Acid (≥99 %, HEPES) from Fisher Scientific was used to buffer the solutions.

For all experiments, equipments (Corning® tubes, syringes, etc.) were pre-cleaned before use with HNO_3 washing (10 %, Fisher, Analytical Grade) then thoroughly rinsed with milliQ water.

Adsorption experiments

The kinetic experiments showed that nickel removal was rapid, and 30 minutes are enough to reach the maximal adsorption. Therefore, a contact time of 180 min, leading to an easier handling, was chosen for all the further experiments. The adsorption experiments were carried out at room temperature in 50 mL Corning© tubes by mixing a fixed amount of adsorbent (0.4 g) with 40 mL of aqueous solution; i.e., 1:100 solid to liquid ratio, buffered at pH 7.0 using HEPES buffer. Aqueous solutions were prepared by dissolving $Ni(NO_3)_2 \cdot 6H_2O$ and $AgNO_3$, respectively, to reach the desired concentrations. The mixture was shaken with an orbital shaker at a speed of 80 rpm during 180 min. All experiments were carried out in duplicate. At the end of adsorption experiments, dispersions were centrifuged at 5000 rpm for 5 min. The supernatant solution was then filtered with Syringe Filters, 0.45µm - Surfactant - Free Cellulose Acetate. The filtrates were acidified with suprapur® HNO_3 at pH < 2 and stored at 4 °C before their analysis.

Nickel retention was studied on all materials (raw and calcined bentonite) over a wide concentration range, from 10 to 130 mg/L, in order to better model the adsorption mechanisms. Silver retention was studied on raw-Be and Be550 only, because these two materials provided the best retention results towards nickel. The studied concentration range was 10 to 130 mg/L. These values were chosen to frame the real contaminant levels in the most contaminated considered effluent (around 80 and 42 mg/L for nickel and silver, respectively).

Nickel and silver competition on raw-Be and Be550 were studied in binary-component system. The experiments were carried out at a 1:1 ratio of Ni:Ag, with nickel and silver concentrations equally ranging between 10 to 130 mg/L.

Nickel and silver retention on raw-Be and Be550 were studied in natural effluents. Effluents from the brassware industry (A) and effluents from Sebou (S1, S2) and Fez (F1, F2) rivers were also tested in this study. Effluent from brassware industry was directly collected from the rinsing baths before discharge in Fez river. The effluents from Fez and Sebou rivers were collected downstream from Fez city and downstream from the confluence with Fez river respectively, either during a period of brassware fabrication (F1 and S1) or during a non-working day (F2 and S2). The composition of each effluent is shown in Table 1.

Table 1. Physico-chemical characterization of the tested effluents: effluent from brassware industry (A), Fez (F1 and F2) and Sebou (S1 and S2) rivers. Index 1 refers to a period of brassware fabrication and index 2 refers to a non-working day.

	Ni (µg/L)	**RSD** %**	**Ag (µg/L)**	**RSD** %**	**DOC (mg/L)**	**SD*** (mg/L)**	**pH**
A	$80.3 \cdot 10^3$	1.3	$41.7 \cdot 10^3$	0.31	80.7	0.18	8.55
F1	214.6	7.2	94.3	1.8	28.8	0.4	7.12
F2	59.5	1.4	51.1	1	19.4	0.2	6.67
S1	122.8	1.4	28.9	2.4	9.2	0.14	7.11
S2	20.4	2.6	5.1	1.1	7.3	0.04	6.96
EQS*	20	-	5	-	-	-	-

* EQS: Environmental Quality Standard.
** RSD: Relative Standard Deviation.
*** SD: Standard Deviation.

In order to examine the reusability of the adsorbent, the used material was agitated with 10 mL of 0.05 mol/L HNO_3 for 30 min, then washed three times with milliQ water to remove the excess of trace metals and acidity. Finally, the adsorbent was dried at 60 °C

for 24 hours. Then, nickel and silver adsorption were performed again, with equal concentrations of 65 mg/L. The regeneration cycle was repeated five times.

For all experiments, trace metal concentrations were measured by inductively coupled plasma-atomic emission spectroscopy on an ICP-AES (Iris Intrepid IIXDL ICP-AES). All samples were analyzed at least twice, and the duplicate determinations agreed within 5%.

Adsorption Models

Equilibrium isotherms for nickel and silver were obtained by performing batch adsorption studies. The amount of the metal ion adsorbed per unit mass of the adsorbent at equilibrium, q_e (mg/g), and the adsorption rate (%) were calculated from the expressions:

$$q_e = \frac{(C_0 - C_e)}{m} \times V \qquad (1)$$

$$\% \text{ Adsorption} = \frac{(C_0 - C_e)}{C_0} \times 100 \qquad (2)$$

where C_0 (mg/L) is the metal ion initial concentration, C_e (mg/L) is the metal ion concentration at equilibrium, m is the mass of adsorbent (g) and V is the volume of solution (L).

The adsorption data were analyzed using Langmuir [15] and Freundlich [16] models. Langmuir model is based on a homogeneous surface with a finite number of identical sites. It also assumes that there is no interaction between the adjacent sites. Langmuir equation is expressed as:

$$\frac{C_e}{q_e} = \frac{1}{K_L q_m} + \frac{C_e}{q_m} \qquad (3)$$

where q_m (mg/g) refers to the maximum adsorption capacity and K_L (L/mg) is the Langmuir constant.

Freundlich model supposes that adsorption occurs onto a heterogeneous surface. This model is expressed by the following equation:

$$q_e = K_F C_e^{1/n} \qquad (4)$$

Freundlich linearization follows:

$$\text{Ln } q_e = \text{Ln } K_F + \frac{1}{n} \text{Ln } C_e \qquad (5)$$

where K_F and n are Freundlich constants related to the adsorption capacity and the strength of adsorption respectively.

The rate of equilibrium adsorption reduction (Δ) was another considered parameter. [17] It is the ratio of the difference between non-competitive equilibrium adsorption and competitive equilibrium adsorption to non-competitive adsorption observed at equilibrium:

$$(\Delta)\% = \frac{(q_i m - q_i mix)}{q_i m} \times 100 \qquad (6)$$

where $q_i m$ (mg/g) and $q_i mix$ (mg/g) are the maximum adsorption capacity of i species in the single component system and binary component system, respectively.

Results and discussion

Physico-chemical characterization of the considered materials

All raw samples presented a low organic content (< 0.04 wt.%). The pH values of the bentonite samples (raw-Be, Be550 and Be750) were measured to be 9.3, 7.3 and 6.4, respectively (Table 2). Zeta potential (ZP) was always negative. Be550 and Be750 have a more acidic character, probably due to the occurring dehydroxylation process [18].

Table 2. Physico-chemical properties of bentonite samples (Number of analyzed samples = 3).

	raw-Be	Be550	Be750
pH	9.3 ± 0.1	7.3 ± 0.2	6.4 ± 0.15
ZP* (mV)	-16.5 ± 0.15	-25 ± 1.4	-33.5 ± 0.7
S_{BET} ** **(m^2/g)**	14.5 ± 0.43	37.1 ± 0.3	29.9 ± 0.31

* ZP: zeta potential.
** S_{BET}: surface area calculated by the BET method.

The mineralogical composition determined by X-ray diffraction of the raw bentonite (Raw-Be) and calcined bentonite are presented in Fig.1. The phases were identified using X'Pert Highscore software through the JCPDS database. The studied bentonites mostly consist of montmorillonite (Mt) and also contain feldspars (F) and small amounts of crystalline phases in the form of impurities quartz (Q). For Raw-Be, the characteristic peaks of montmorillonite (the major compound of bentonite) at Bragg angles 2θ = 5.9° (14.9 Å), 20.2° (4.3 Å), 34.1° (2.6 Å), 35.8° (2.5 Å) and 62.2° (1.49 Å) were encountered. Feldspars peaks (2θ = 13.6° (6.5 Å) and 27.7° (3.2 Å)) and quartz peak (2θ = 26.6° (3.3 Å)) could also be observed. Through the evaluation of bentonite after thermal treatment, a structural change can be noticed, with the shift of the characteristic montmorillonite peak at Bragg angles 2θ = 6.7°. D-spacing series of smectites are similar for calcined bentonite (550-750 °C) with reflection (d_{001}) at d = 13.6 Å-13.9 Å. Dehydroxylation and dehydration processes occurring during the calcination process may be followed by cation movement within the octahedral sheet. [19, 20] Therefore, it can be concluded that the structural and basal spacing changes caused by thermal treatment acted on the hydration capacity of clays, provoking interlayer collapse and a transformation to an illite structure type.

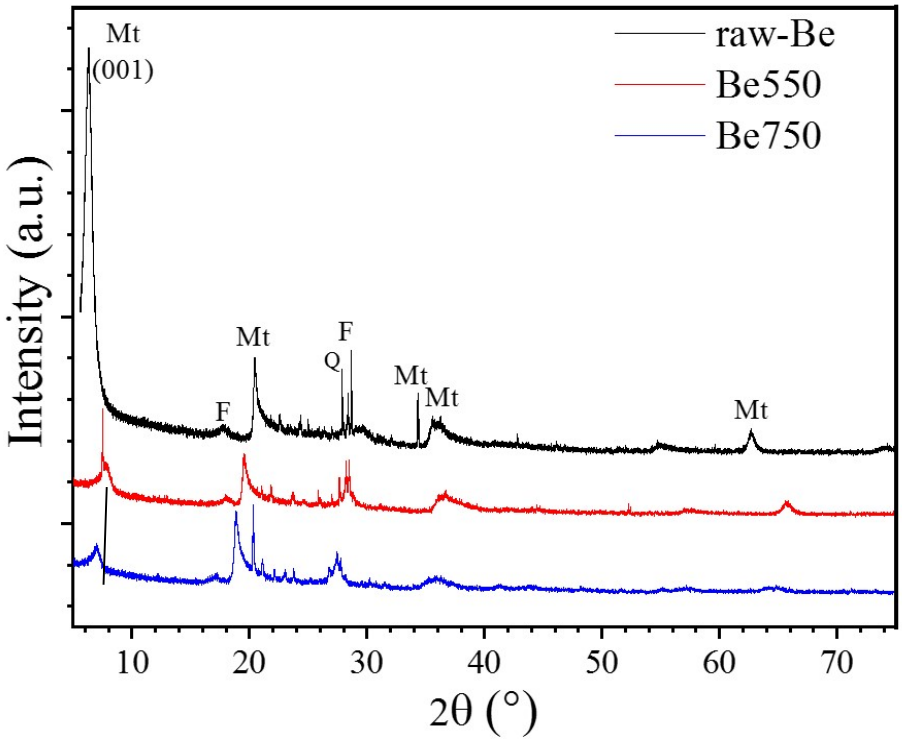

Figure 1. Powder XRD profiles of raw-Be, Be550 and Be750. (Mt: Montmorillonite, F: Feldspar, Q: Quartz).

FTIR spectra of the natural and calcined bentonite (Fig.2) showed infra-red bands located in the range of 400-1100 cm^{-1} corresponding to the stretching and deformation modes of Si-O-Si and Si-O-Al. [12, 19, 21, 22] The peak at 517 cm^{-1} is attributed to the Si-O-Al (related to the octahedral sheet) vibration band. [22] The strong band at 1000 cm^{-1} of raw-Be can be attributed to a Si-O stretching vibration of the condensed phase, affected by Si-O-H deformation vibration band. [23] The presence of adsorbed water is evidenced by the band at 1635 cm^{-1}, characteristic of the bending vibration of H_2O, while the band at 3396 cm^{-1} corresponds to water stretching vibration band, and 3623 cm^{-1} to the stretching vibration of structural OH groups. [24]

Upon thermal treatment, the intensity of all the bands related to the water and hydroxyl groups presence (1635, 3396 and 3623 cm^{-1}) strongly decreased in the spectrum of

Be550. Moreover, these bands disappeared for bentonite calcined at 750 °C, as a proof of the dehydroxylation and decomposition of the structure of the bentonite samples, respectively. The thermal treatment also caused an important evolution of the strong Si-O stretching vibration band present in the raw-Be spectrum at 1000 cm^{-1}.

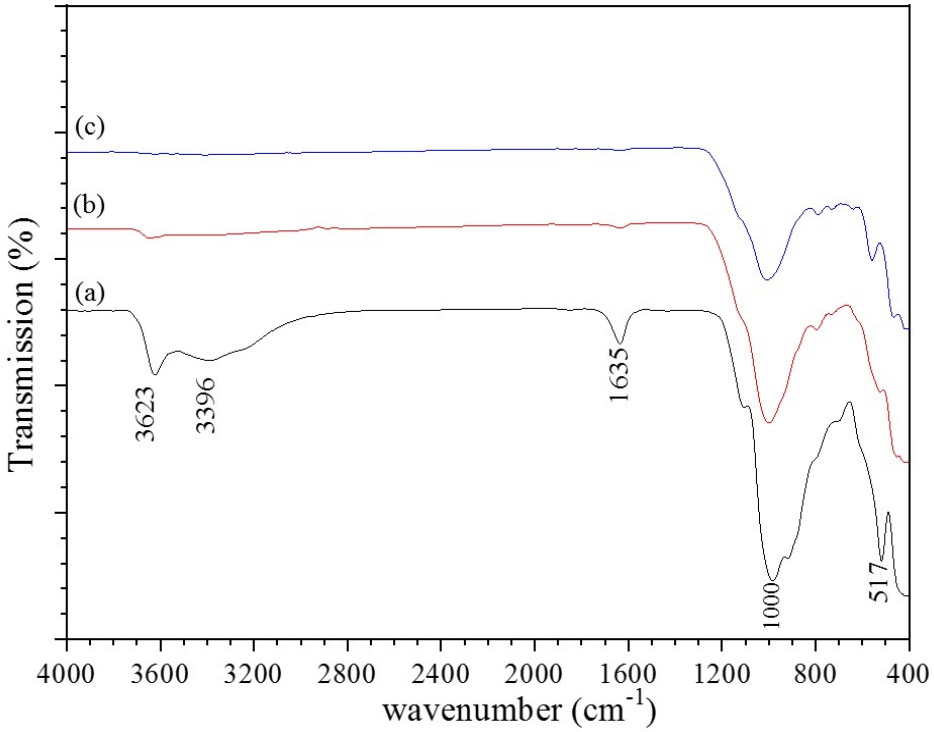

Figure 2. FTIR spectra of raw-Be (a), Be550 (b) and Be750 (c).

The thermogravimetric curves showed a total weight loss of 12.6 %; 4.5 % and 4 % for raw-Be; Be550 and Be750 respectively (Fig.3). The raw sample showed the greatest loss of mass at 250 °C, due to the removal of hydroscopic and interlayer cation solvating water [25, 26], in agreement with FTIR observation.

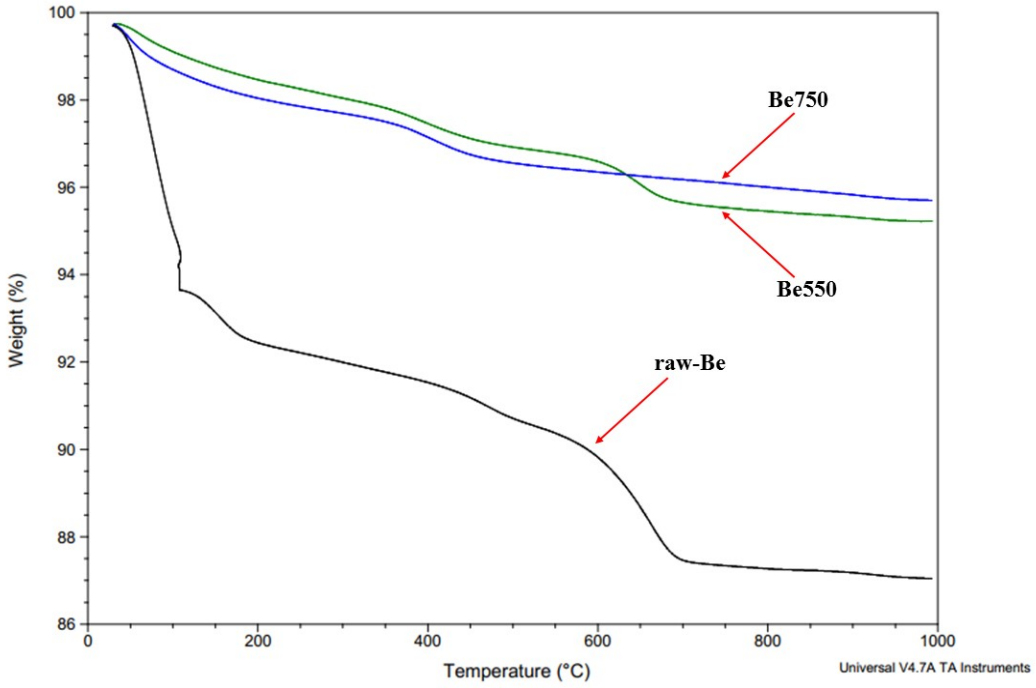

Figure 3. TGA curves of raw-Be, Be550 and Be750.

Morphology and characterization of the considered materials

The morphology of raw (Fig. 4a) and calcined bentonite (Figs. 4b to 4c) showed an irregularity of the particles forming aggregates. For raw-Be, SEM pictures showed the classical general appearance of the montmorillonite, essentially constituted of sheets. [27, 28]

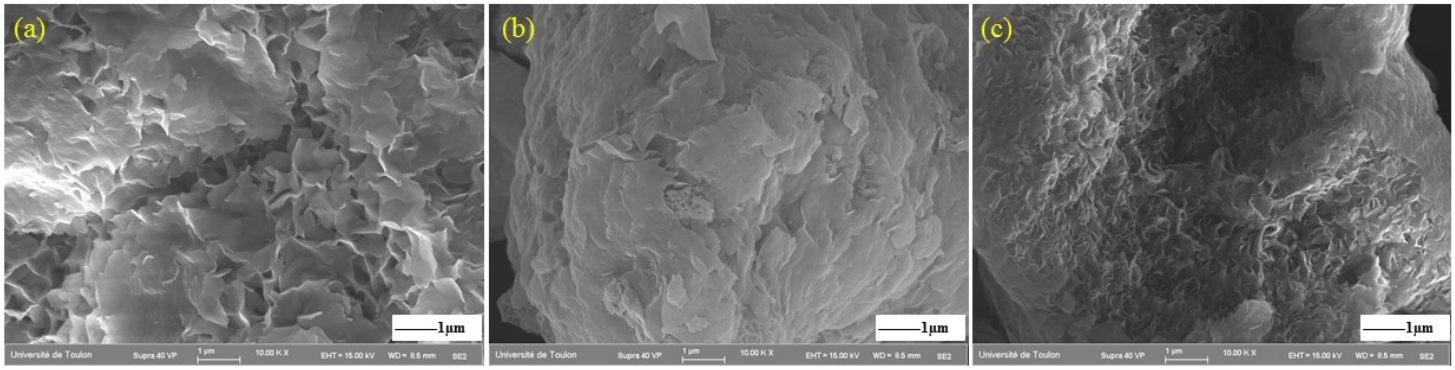

Figure 4. SEM images of raw-Be (a) Be550 (b) and Be750 (c).

The obtained results (Table 2) demonstrated a modification of the specific surface area (BET) with the heating treatment. When considering Be550 and Be750, an increase in the BET surface area (37.1 m^2/g and 29.9 m^2/g, respectively) was measured, which corresponds to an increase of 61 % and around 52 %, in comparison with raw-Be, respectively. In the literature, it was already demonstrated that thermal treatment improved bentonite surface area, though the tested temperatures were lower [12] than that or the present study.

In conclusion, as long as a critical temperature is not exceeded, the heating treatment was demonstrated to induce a positive impact on bentonite structure, and especially on specific surfaces.

Nickel and silver retention in single-component systems

The equilibrium isotherms in single component systems are presented in Figs. 5a to 5d. The best nickel retention capacity (5.6 mg/g) was obtained for raw-Be and the lowest one for Be750. The obtained results on Be550 (~4.6 mg/g) and Be750 (~2.1 mg/g) did not fully follow the variation of specific surface with heating treatment. High heating treatment leads to the desorption of hydration and interlayer water which decreases the interlayer spaces of bentonite. Therefore, Be750 is more densely packed, as proven with FTIR and SEM analyses. Thus, this phenomenon tends to decrease the amount of nickel adsorbed for Be750. Nickel ions adsorption decreased by 61% when considering the materials submitted to thermal treatment above 550 °C. This suggests that the heating above the dehydroxylation temperature collapses the structure due to the destruction of the bentonite layered structure. [29] It can be concluded that the heating temperature should not be higher than 550 °C to keep bentonite high-performance adsorption properties.

Adsorption isotherms were modeled by Langmuir (Eq (3)) and Freundlich models (Eq (5)). Raw-Be and Be550 were best fitted by Langmuir model, while Be750 was best fitted by Freundlich model (Table 3), which confirmed the heterogenous sites on the Be750. The maximal retention capacities obtained from modelling were 5.5, 4.3 and 2.2 mg/g for raw-Be, Be550 and Be750, respectively. The significantly decreased adsorption capacity of the bentonite calcined at 750 °C was clearly remarked. This can be explained by the transition to a multilayer adsorption, as implied by Freundlich modelling. Such multilayer adsorption could lead to a decrease in surface area of micropores and hence, the decrease in the adsorption sites' availability.

The experimental maximal capacities obtained in this work were compared to those of other studied bentonite as well as materials of similar structure and composition (Table 4). Looking at the literature, raw-Be and Be550 demonstrated a retention ability towards nickel in the upper range.

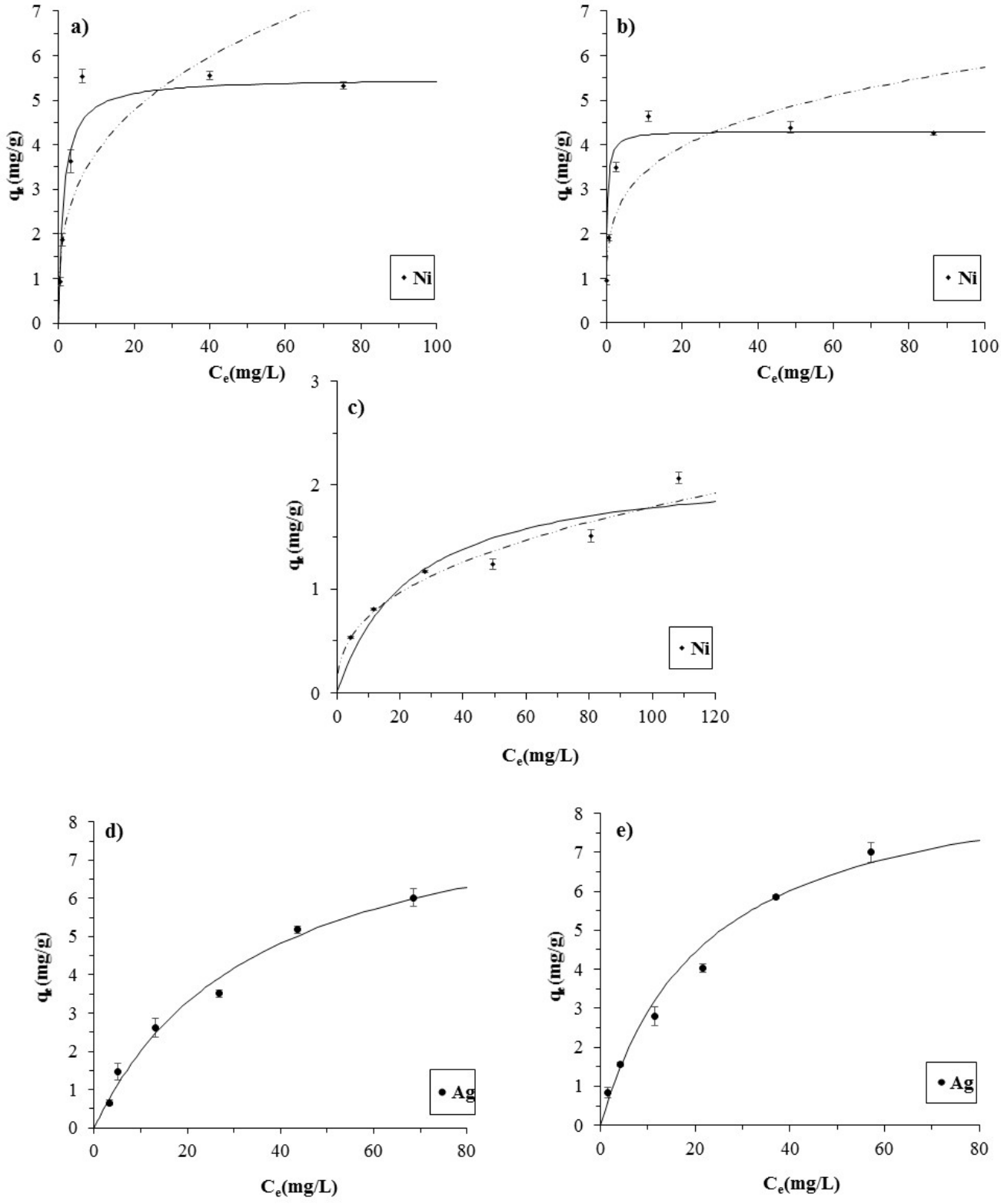

Figure 5. Equilibrium isotherms for nickel adsorption onto raw-Be (a), Be550 (b) and Be750 (c) as well as equilibrium isotherms for silver adsorption onto raw-Be (d), Be550 (e). Dash-dotted lines represent Freundlich fitting and solid lines Langmuir fitting.

Table 3. Langmuir and Freundlich parameters for nickel retention onto raw-Be, Be550, and Be750 as well as silver retention onto raw-Be and Be550 in single and binary component systems.

System	Metal	Model	Parameter	Adsorbent		
Single-component system	**Ni**	Langmuir		raw-Be	Be550	Be750
			q_m (mg/g)	5.5	4.3	2.2
			K_L	0.75	4.6	0.04
		Freundlich	R^2	0.998	0.994	0.914
			1/n	0.32	0.23	0.38
			K_F	1.82	1.98	0.3
			R^2	0.755	0.789	0.969
	Ag	Langmuir	q_m (mg/g)	9.1	9.3	-
			K_L	0.028	0.045	-
			R^2	0.946	0.954	-
Binary-component system	**Ni (Ni-Ag)**	Langmuir	q_{imix}	3.8	2.8	-
			K_L	0.09	0.15	-
			R^2	0.984	0.971	-
			q_{imix}/q_{im}	0.699	0.645	-
			Δ (%)	30	35	-
	Ag (Ag-Ni)		q_{imix}	5.9	6.9	-
			K_L	0.02	0.03	-
			R^2	0.809	0.848	-
			q_{imix}/q_{im}	0.654	0.744	-
			Δ (%)	34	26	-

Table 4. Comparison of nickel and silver adsorption capacity by different studied bentonites and materials of structure and composition similar to those studied in the present work.

Metal	Adsorbents	q_m (mg/g)	Reference
Ni	Ca-montmorillonite	4.84	[30]

	Bofe bentonite	1.91	[31]
	Ca-bentonite	6.3	[32]
	K10 montmorillonite clay	2.1	[33]
	Sepiolite	2.24	[34]
	raw-Be	**5.6**	**present study**
	Be550	**4.6**	**present study**
	Be750	**2.1**	**present study**
Ag	Low-rank Turkish Coals	1.86	[35]
	Expanded perlite	8.46	[36]
	Calcareous soils	3.65	[37]
	raw-Be	**6**	**present study**
	Be550	**6.9**	**present study**

The equilibrium isotherm for silver adsorption on raw-Be and Be550 (Figs. 5d and 5e) demonstrated that unlike nickel, silver adsorption followed the variation of the specific surface: 6.0 and 6.9 mg/g, on raw-Be and Be550, respectively. The modelling obtained by Langmuir (Table 3) implies a monolayer adsorption which corroborates a chemisorption for nickel and silver removal onto raw-Be and Be550. Silver modelled retention capacities were higher than that of nickel: 9.1 and 9.3 mg/g for raw-Be and Be550, respectively (Table 3). In any case, bentonite demonstrated its ability to efficiently remove metals in a simple media (Table 4).

The adsorption of silver ions may be affected by ion exchange, which occurs between the metal ions and the amounts of alkali and alkaline-earth metals in bentonite samples (e.g. Ag^{+} can take place of the exchangeable cations such as Na^{+}, Mg^{2+} and K^{+} in

bentonite layer and interposed between the bentonite layers). Besides, silver adsorption may be also due to the fact that heating treatment at 550 °C caused enhancement of aluminum ions (Table SI-1), or hydroxoaluminum cations at the edges, which promotes the interaction with metal ions, as already demonstrated. [12, 38, 39] From these results, it must be underlined that raw-Be and Be550 retention were still in the higher range when compared to other bentonites or materials of similar structure and composition (Table 4).

Nickel and silver retention in binary-component systems

The amounts adsorbed in the single component systems were higher than that in binary component systems (Fig. 6). Nickel retention capacity onto raw-Be and Be550 were 3.6 and 2.8 mg/g, respectively. Silver retention capacity onto raw-Be and Be550 were 4.2 and 4.9 mg/g, respectively. These results followed the same trend as that of single-component systems. It was clear that the presence of another metal led to a competition for the adsorption sites on raw-Be and Be550.

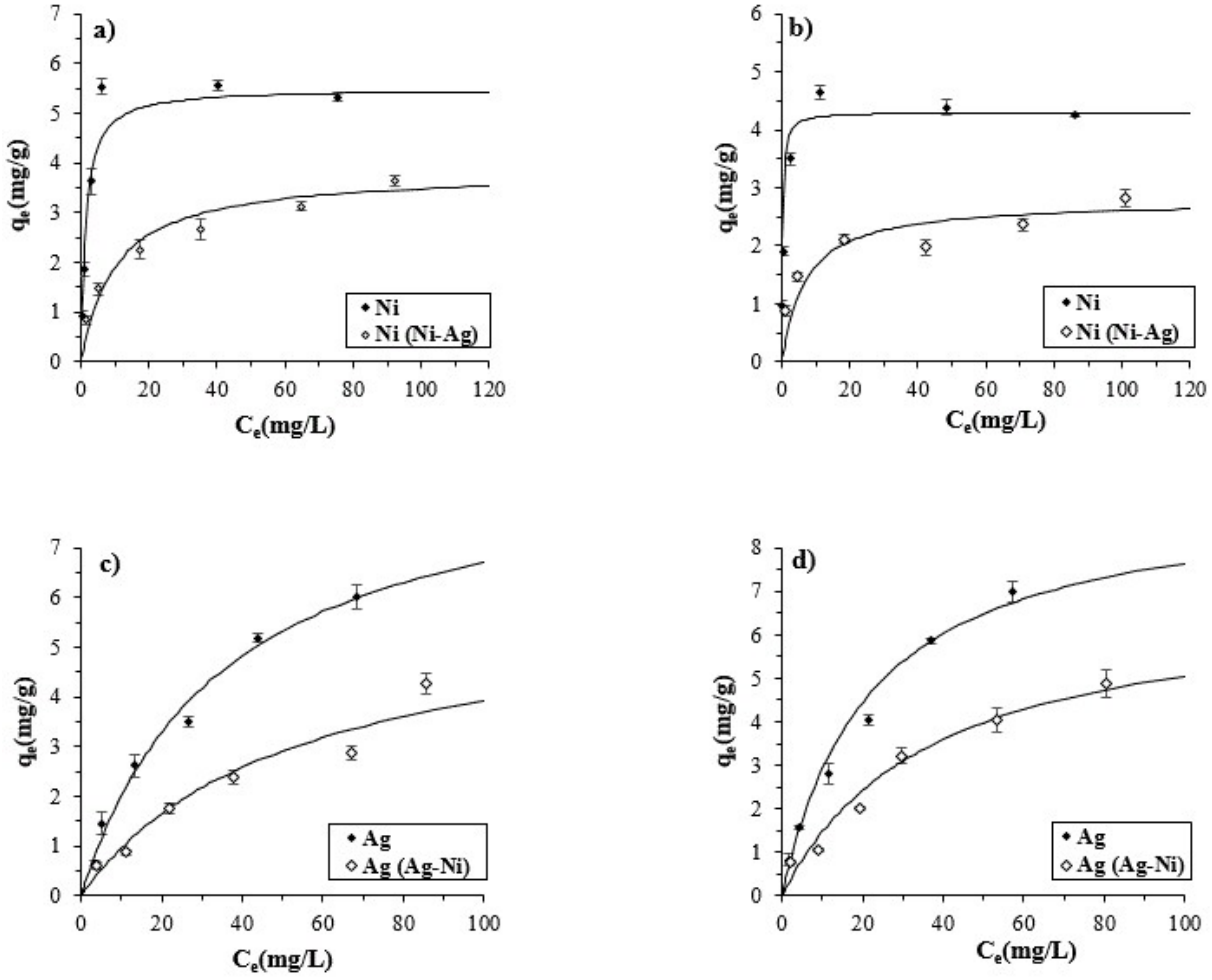

Figure 6. Single and binary adsorption of nickel on raw-Be (a) and Be550 (b) as well as equilibrium isotherms for silver adsorption onto raw-Be (c) and Be550 (d). The solid lines represent the fitting by Langmuir modelling.

Such enhanced competitive effects in binary-components was investigated using the ratio of the maximum adsorption capacity for the metal in the binary-component system (q_{imix}) to the maximum adsorption capacity for the same metal in the single-component (q_{im}) [17, 40]. If $q_{imix}/q_{im} > 1$, the adsorption is promoted in the presence of the other metal ions; if $q_{imix}/q_{im} = 1$, there is no effect and interaction between metal ion i and other metals ions; if $q_{imix}/q_{im} < 1$, the adsorption is decreased by the presence of other metal ions. The values of q_{imix}/q_{im} and the rate of equilibrium adsorption reduction (Δ) are

shown in Table 3. All q_{imix}/q_{im} values were below 1, which confirms the mutual competitive effect of nickel and silver in binary component systems. For raw-Be, the rate of equilibrium adsorption reduction (Δ) (eq(7)) of nickel was diminished by nearly 30% in binary-component system (Ni-Ag), and for (Ag) was decreased by 34% in the (Ag-Ni) system. Likewise, for Be550 in Ni(Ni-Ag) and Ag(Ag-Ni) systems (Δ) this rate was decreased by 35% and 26%, respectively.

Following the previous modelling results, only Langmuir was used (Table 3) to fit the experimental data in binary-system. The high values of correlation coefficients showed that equilibrium data were well-fitted, which corroborates the monolayer adsorption of nickel and silver onto raw-Be and Be550.

Nickel and silver retention in natural effluents

The brassware effluent (A) was characterized by the highest metal levels: 80.3 mg/L of nickel and 41.7 mg/L of silver, respectively (Table 1). The effluents from Fez (F1) and Sebou rivers (S1) during working day were polluted in nickel and silver, though at a lesser extent: 214.6 and 94.3 µg/L, respectively, in Fez river and 122.8 and 28.9 µg/L, respectively, in Sebou river. Fez (F2) and Sebou rivers (S2) during non-working day were the least polluted in nickel and silver: 59.5 and 51.1 µg/L, respectively, in Fez river and 20.4 and 5.1 µg/L, respectively, in Sebou river (Table 1).

The obtained values were compared to environmental quality standards (EQS) concentrations. Nickel and silver concentrations in the studied effluents from Fez and Sebou rivers during working day (F1 and S1) were critically above (up to a 10-fold) the environmental quality standard (EQS) concentrations of nickel (20µg/L) [41] and silver (5µg/L). [42] Nickel and silver concentrations in the studied effluents from Fez and

Sebou rivers during non-working day (F2 and S2) were also exceeding the environmental quality standard (EQS) concentrations, but in a less dramatic extent.

The retention of nickel for the brassware industry effluent (A) by raw-Be and Be550 turned less efficient due to the presence of numerous competing agents. Raw-Be and Be550 retention capacity were 1.2 and 1.5 mg/g respectively for nickel. The difference between the raw and calcined materials was low but in favor of the calcined material.

The removal efficiency of raw-Be and Be550 for both nickel and silver in Sebou and Fez rivers were 100 % (Figs. 7a and 7b). It has to be underlined that even if the tested effluents were less contaminated in metals than the brassware rinsing bath, their metals' content was important. Yet, both materials demonstrated a good efficiency and ability for removal nickel and silver such complex and contaminated media.

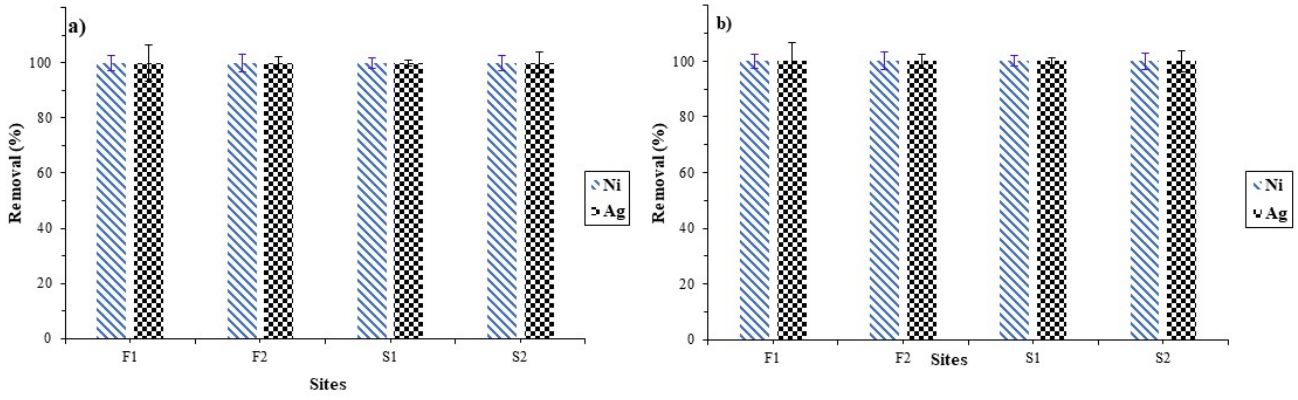

Figure 7. Adsorption of nickel and silver from natural effluent onto raw-Be (a) and Be550 (b). Samples are from Fez (F1 and F2) and Sebou (S1 and S2) rivers, in which index 1 refers to a period of brassware fabrication and index 2 refers to during a non-working day.

Regeneration study

The regeneration of raw-Be and Be550 adsorbents is very important from an environmental and economical point of view if an industrial application is targeted. The impact of regeneration cycles on efficiency removal (Fig.8) highlighted that from the

first cycle of regeneration until the fifth one, nickel removal efficiency on raw-Be decreased by 15 % whereas only a slight decrease (3 %) was observed for Be550. Concerning silver, both raw-Be and Be550 removal efficiency diminished, by 24 % and 14 %, respectively, which remained quite low. Therefore, the regenerated Be550 demonstrated a high efficiency, sustainable in time.

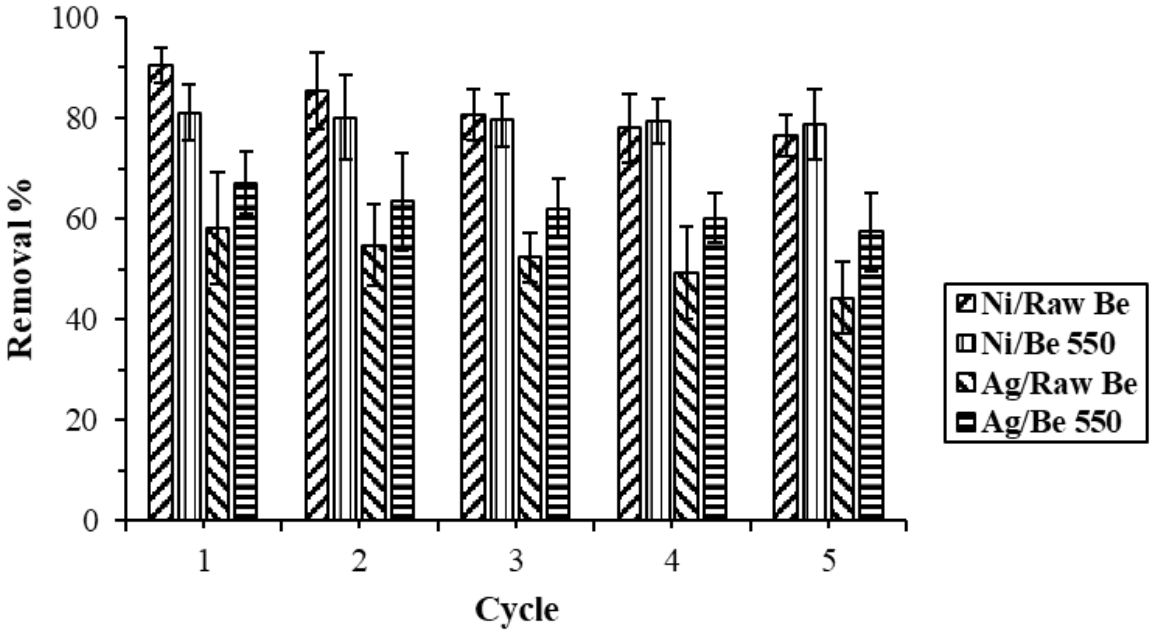

Figure 8. Regeneration of raw-Be and Be550 in the retention of nickel and silver.

Conclusions

In this paper, a natural bentonite from northeastern of Morocco was studied before and after modification through heating treatment at two different temperatures: 550 and 750 °C. The obtained results showed that by calcination at these two different temperatures for 6 hours, various transformations occurred, especially an enhancement of the surface area with temperature.

The adsorption experiments carried out have shown that raw-Be and Be550 materials demonstrated a noticeable retention ability towards nickel, but also silver, taken separately or as a binary-component system. Equilibrium studies revealed that nickel maximum adsorption capacity (5.5 mg/g) and silver maximum adsorption capacity (6.9 mg/g) were noticeably higher than materials of similar composition. The adsorption isotherms were better represented by Langmuir model. The use of raw-Be and Be550 were then successfully tested in industrial effluents: brassware industry effluent as well as river effluents, demonstrating the possible use of this worldwide materials in wastewaters treatment. Finally, the regeneration study revealed a net benefit for Be550. So, its use in an industrial process is conceivable. In complex media, the calcined material demonstrated its enhanced properties and skills, highlighting the positive effect of heating treatment, as far as bentonite is concerned.

Acknowledgement

The authors wish to thank Mr. M. Akhazzane (USMBA, Morocco), Mr. A. Fahs and Mr. P. Carriere (Toulon University, France) for easing the access to some analytical apparatus and their help during the measurements. The authors also wish to thank Academy of Finland.

References

[1] Ranelovic, M. S., Purenovic, M. M., Matovic, B. Z., Zarubica, A. R., Momčilovic, M. Z., & Purenovic, J. M. (2014) Structural, textural and adsorption characteristics of bentonite-based composite. *Microporous and Mesoporous Materials*, *195*: 67–74. https://doi.org/10.1016/j.micromeso.2014.03.031

[2] John. W. Anthony, Richard. A .Bideaux, Kenneth. A. Bladh, M. C. N. (1995) *Handbook of Mineralogy II.Silica, Silicates*. *Mineral Data Publishing* (Vol. 2).

[3] Murray, H. H. (2006) Chapter 6 Bentonite Applications. *Developments in Clay Science*, *2* (C): 111–130. https://doi.org/10.1016/S1572-4352(06)02006-X

[4] Chamley, H. (1989) Clay Formation Through Weathering. *Clay Sedimentology*, 21–50. https://doi.org/10.1007/978-3-642-85916-8_2

[5] Decarreau, A., & Mat, A. D. (1990) *Clay materials: Structure, properties and applications.Société française de Minéralogie et de Cristallographie et Groupe Français des Argiles*.

[6] Liang, X., Lu, Y., Li, Z., Yang, C., Niu, C., & Su, X. (2017) Bentonite/carbon composite as highly recyclable adsorbents for alkaline wastewater treatment and organic dye removal. *Microporous and Mesoporous Materials*, *241*: 107–114. https://doi.org/10.1016/j.micromeso.2016.12.016

[7] Koch, D. (2002) Bentonites as a basic material for technical base liners and site encapsulation cut-off walls. *Applied Clay Science*, *21*: 1–11.

[8] Chen, W. J., Hsiao, L. C., & Chen, K. K. Y. (2008) Metal desorption from copper(II)/nickel(II)-spiked kaolin as a soil component using plant-derived saponin biosurfactant. *Process Biochemistry*, *43* (5): 488–498. https://doi.org/10.1016/j.procbio.2007.11.017

[9] Steudel, A., Batenburg, L. F., Fischer, H. R., Weidler, P. G., & Emmerich, K. (2009) Alteration of non-swelling clay minerals and magadiite by acid activation. *Applied Clay Science*, *44* (1–2): 95–104. https://doi.org/10.1016/j.clay.2009.02.001

[10] Zhang, Y., Zhao, Y., Zhu, Y., Wu, H., Wang, H., & Lu, W. (2012) Adsorption of mixed cationic-nonionic surfactant and its effect on bentonite structure. *Journal of Environmental Sciences (China)*, *24* (8): 1525–1532. https://doi.org/10.1016/S1001-0742(11)60950-9

[11] Saleem, M., Tanveer, F., Ahmad, A., & Gilani, S. A. (2018) Correlation between shoulder pain and functional disability among nurses. *Rawal Medical Journal*, *43* (3): 483–485. https://doi.org/10.1002/app

[12] Bertagnolli, C., Kleinübing, S. J., & Gurgel, M. (2011) Preparation and characterization of a Brazilian bentonite clay for removal of copper in porous beds. *Applied Clay Science*, *53* (1): 73–79. https://doi.org/10.1016/j.clay.2011.05.002

[13] Oliveira, M. F., da Silva, M. G. C., & Vieira, M. G. A. (2019) Equilibrium and kinetic studies of caffeine adsorption from aqueous solutions on thermally modified Verde-lodo bentonite. *Applied Clay Science*, *168* (December 2018): 366–373. https://doi.org/10.1016/j.clay.2018.12.011

[14] Krupskaya, V., Novikova, L., Tyupina, E., Belousov, P., Dorzhieva, O., Zakusin, S., … Belchinskaya, L. (2019) The influence of acid modification on the structure of montmorillonites and surface properties of bentonites. *Applied Clay Science*, *172* (February): 1–10. https://doi.org/10.1016/j.clay.2019.02.001

[15] Langmuir, I. (1918) The adsorption of gases on plane surfaces of glass, mica and platinum. *Journal of the American Chemical society*, *345* (1914): 1361–1403.

[16] Freundlich, H. (1906) Über die Adsorption in Lösungen. *Zeitschrift für physikalische Chemie*, *57* (4): 385–470.

[17] Zhi-rong, L., & Shao-qi, Z. (2009) Adsorption of copper and nickel on Na-bentonite. *Process Safety and Environmental Protection*, *88* (1): 62–66. https://doi.org/10.1016/j.psep.2009.09.001

[18] Vieira, M. G. A., Neto, A. F. A., Gimenes, M. L., & Silva, M. G. C. (2010) Removal of nickel on Bofe bentonite calcined clay in porous bed. *Journal of Hazardous Materials*, *176*: 109–118. https://doi.org/10.1016/j.jhazmat.2009.10.128

[19] Ayari, F., Srasra, E., & Trabelsi-Ayadi, M. (2005) Characterization of bentonitic clays and their use as adsorbent. *Desalination*, *185* (1–3): 391–397. https://doi.org/10.1016/j.desal.2005.04.046

[20] Jaynes, W. F., & Bigham, J. M. (1987) Charge reduction, octahedral charge , and lithium retention in heated , li-saturated smectites. *Clays and Clay Minerals journal*, *35* (6): 440–448.

[21] Xu, W., Johnston, C. T., Parker, P., & Agnew, S. E. (2000) Infrared study of water sorption on Na- , Li- , Ca- , and Mg-exchanged (SWy- 1 and SAz- 1) Montmorillonite. *Clays' and Clay Minerals*, (1): 120–131.

[22] Er-ramly, A. (2014) Physicochemical and Mineralogical Characterization of Moroccan Bentonite of Trebia and Its Use in Ceramic Technology. *American Journal of Physical Chemistry*, *3* (6): 96. https://doi.org/10.11648/j.ajpc.20140306.12

[23] G. Socrates (2001) Infrared and Raman Characteristic Group Frequencies. Tables and Charts. *John Wiley and Sons*.

[24] Farmer, V. C. (1974) Infrared spectra of minerals. *Mineralogical Society Monograph 4*, 539.

[25] Kok, M. V. (2002) Thermogravimetry of selected bentonites. *Energy Sources*, *24* (10): 907–914. https://doi.org/10.1080/00908310290086833

[26] Zaitan, H., Bianchi, D., Achak, O., & Chafik, T. (2008) A comparative study of the adsorption and desorption of o-xylene onto bentonite clay and alumina. *Journal of Hazardous Materials*, *153* (1–2): 852–859. https://doi.org/10.1016/j.jhazmat.2007.09.070

[27] Uddin, M. K. (2017) A review on the adsorption of heavy metals by clay minerals , with special focus on the past decade. *Chemical Engineering Journal*, *308*: 438–462. https://doi.org/10.1016/j.cej.2016.09.029

[28] Shichi, T., & Takagi, K. (2000) Clay minerals as photochemical reaction fields. *Journal of Photochemistry and Photobiology C: Photochemistry Reviews*, *1* (2): 113–130. https://doi.org/10.1016/S1389-5567(00)00008-3

[29] Bergaya, F., Theng, B. K. G., & Lagaly, G. (2006) Modified Clays and Clay MineralsIn . *Developments in Clay Science* (Elsevier., Vol. 1, p. 261).

[30] Pablo, L. De, Chávez, M. L., & Abatal, M. (2011) Adsorption of heavy metals in acid to alkaline environments by montmorillonite and Ca-montmorillonite. *Chemical Engineering Journal*, *171* (3): 1276–1286. https://doi.org/10.1016/j.cej.2011.05.055

[31] Vieira, M. G. A., Neto, A. F. A., Gimenes, M. L., & Silva, M. G. C. (2010) Sorption kinetics and equilibrium for the removal of nickel ions from aqueous phase on calcined Bofe bentonite clay. *Journal of Hazardous Materials*, *177* (1–3): 362–371. https://doi.org/10.1016/j.jhazmat.2009.12.040

[32] Alvarez-Ayuso and Garcia-Sanchez (2003) Removal Of Heavy Metals From Waste Waters By Natural And Na-Exchanged Bentonites. *Clays and Clay Minerals*, *51* (5): 475–480. https://doi.org/10.1346/CCMN.2003.0510501

[33] Carvalho, W. A., Vignado, C., & Fontana, J. (2008) Ni (II) removal from aqueous effluents by silylated clays. *Hazardous Materials*, *153*: 1240–1247. https://doi.org/10.1016/j.jhazmat.2007.09.083

[34] Ansanay-Alex, S., Lomenech, C., Hurel, C., & Marmier, N. (2012) Adsorption of nickel and arsenic from aqueous solution on natural sepiolite. *International Journal of Nanotechnology*, *9* (3–7): 204–215. https://doi.org/10.1504/IJNT.2012.045327

[35] Karabakan, A., Karabulut, S., Denizli, A., & Yürüm, Y. (2003) Removal of Silver (I) from Aqueous Solutions with Low-rank Turkish Coals. *Adsorption Science & technology*, (November): 135–144. https://doi.org/10.1260/026361704323150917

[36] Ghassabzadeh, H., Mohadespour, A., Torab-mostaedi, M., Zaheri, P., Ghannadi, M., & Taheri, H. (2010) Adsorption of Ag , Cu and Hg from aqueous solutions using expanded perlite. *Journal of Hazardous Materials*, *177* (1–3): 950–955. https://doi.org/10.1016/j.jhazmat.2010.01.010

[37] Rahmatpour, S., Shirvani, M., & Mosaddeghi, M. R. (2017) Retention of silver nano-particles and silver ions in calcareous soils : Influence of soil properties. *Journal of Environmental Management*, *193*: 136–145. https://doi.org/10.1016/j.jenvman.2017.01.062

[38] El Ouardi, Y., Branger, C., Toufik, H., Laatikainen, K., Ouammou, A., & Lenoble, V. (2020) An insight of enhanced natural material (calcined diatomite) efficiency in nickel and silver retention: application to natural effluents. *Environmental Technology & Innovation*, *18*: 100768. https://doi.org/https://doi.org/10.1016/j.eti.2020.100768

[39] Li, C., Zhong, H., Wang, S., Xue, J., & Zhang, Z. (2015) A novel conversion process for waste residue: Synthesis of zeolite from electrolytic manganese residue and its application to the removal of heavy metals. *Colloids and Surfaces A: Physicochemical and Engineering Aspects*, *470*: 258–267. https://doi.org/10.1016/j.colsurfa.2015.02.003

[40] Mohan, D., & Singh, K. P. (2002) Single- and multi-component adsorption of cadmium and zinc using activated carbon derived from bagasse F an agricultural waste $. *Water Research*, *36*: 2304–2318.

[41] EU (2008) Directive 2008/105/EC of the European Parliament and of the Council of 16 December 2008 on environmental quality standards in the field of water policy, amending and subsequently repealing Council Directives 82/176/EEC, 83/513/EEC,

84/156/EEC,84/491/EEC,. *Official Journal of the European Union*, L348/84-L348/97. https://doi.org/http://eur-lex.europa.eu/legal-content/EN/TXT/?uri=celex:32008L0105

[42] Vorkamp, K., & Sanderson, H. (2016) *European Environmental Quality Standards (EQS) Variability Study: Analysis of the variability between national EQS values across Europe for selected Water Framework Directive River Basin-Specific Pollutants*. *Aarhus University, DCE – Danish Centre for Environment and Energy*.